the profile exhibits two distinct 'slow etching' crystal planes: (01$\bar{1}$) and (111)B. This observation is consistent with the work of Coldren *et al.*[4] on the sensitivity of the etch rate of InP in HCl to the crystal orientation.

The profile in Fig. 2 was obtained using a mixture of 1(HCl): 3(H_3PO_4) (again the grating orientation is (011)). In this case the profile is rectangular with a depth of $\simeq$2000 Å. Here, the etched depth is not limited by the formation of intersecting slow-etching planes, and the rectangular profile produced is particularly attractive for use in second-order DFB lasers since a straightforward Fourier analysis shows it to contain $\simeq$1270 Å of the desired 0·23 μm period harmonic component (the mark/space ratio was taken to be $\simeq$ 1/3). By comparison the commonly used triangular profile[3] contains only 666 Å of this component.

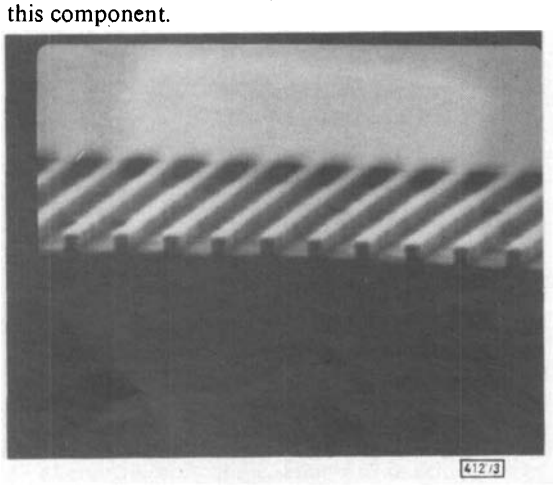

Fig. 3 *As Fig. 1, etched in 1(HCl): 1(CH_3COOH)*
Depth $\simeq$ 2000 Å

A rectangular profile was also achieved using 1(HCl): 1(CH_3COOH) as the etchant. Fig. 3 shows the cross-section of a grating formed in this etchant—again the depth is $\simeq$2000 Å.

A particular advantage of the use of electron-beam-exposed gratings is that, by varying the exposure dose, different groove mark/space ratios can be obtained. Together with controlled over-etching of the SiO_2, this has allowed us to fabricate nearly sawtooth gratings, containing virtually no second-harmonic Fourier component (Fig. 4). The etchant used was 1(HBr):1(CH_3COOH) and in this case the gratings were aligned in the (01$\bar{1}$) direction. The grating depth, which is limited by the formation of (111)A planes, is $\simeq$3200 Å.

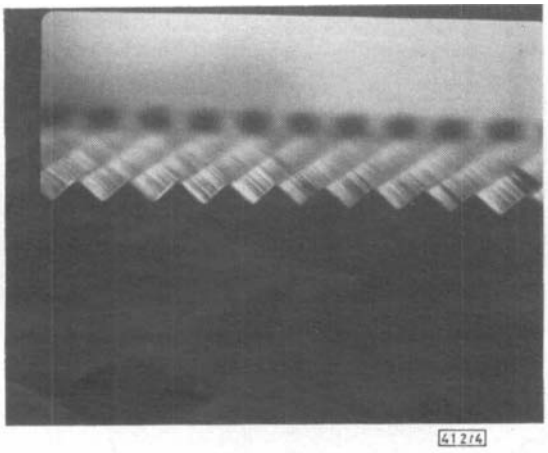

Fig. 4 *As Fig. 1, etched in 1(HBr):(CH_3COOH)*
Depth $\simeq$ 3000 Å

In conclusion, we have demonstrated a submicrometre bilevel process for the production of semiconductor diffraction gratings and have fabricated a range of new grating profiles in InP using this technique. These profiles, having varied Fourier harmonic spectra, should permit the production of more efficient optoelectronic grating devices.

Acknowledgments: The authors thank C. Dix for electron-beam exposure of the grating patterns, P. Rodgers for assistance with the dry etching and B. Wakefield for SEM evaluation. They also acknowledge the Director of Research, British Telecom, for permission to publish this letter.

L. D. WESTBROOK
A. W. NELSON
P. J. FIDDYMENT

British Telecom Research Laboratories
Martlesham Heath, Ipswich, Suffolk IP5 7RE, England

9th November 1983

References

1 UTAKA, K., AKIBA, S., SAKAI, K., and MATSUSHIMA, Y.: 'Room-temperature CW operation of distributed-feedback buried-heterostructure InGaAsP/InP lasers emitting at 1·57 μm', *Electron. Lett.*, 1981, **17**, pp. 961–962

2 TANBUN-EK, T., ARAI, S., KOYAMA, F., KISHINO, K., YOSHIZAWA, S., WATANABE, T., and SUEMATSU, Y.: 'Low-threshold current CW operation of GaInAsP/InP buried-heterostructure distributed-Bragg-reflector laser emitting at 1·5–1·6 μm', *ibid.*, 1981, **17**, pp. 967–968

3 WESTBROOK, L. D., NELSON, A. W., and DIX, C.: 'High-quality InP surface corrugations for 1·55 μm InGaAsP DFB lasers fabricated by electron-beam lithography', *ibid.*, 1982, **18**, pp. 863–865

4 COLDREN, L. A., FURAYA, K., MILLER, B. I., and RENTSCHLER, J. A.: 'Combined dry and wet etching techniques to form planar (011) facets in InGaAsP/InP double-heterostructures', *ibid.*, 1982, **18**, pp. 235–237

PERFORMANCE OF FH-MFSK CELLULAR MOBILE RADIO IN THE PRESENCE OF NONSYNCHRONOUS USERS

Indexing terms: Telecommunication, Synchronisation, Mobile radio systems

Monte Carlo simulation of an FH-MFSK spread-spectrum cellular mobile radio system in the presence of nonsynchronous users is presented. Impairments such as short-term and shadow fading are introduced. Performance curves showing the number of simultaneous users the system can accept are given. Both clustering and no-clustering strategies are considered.

Introduction: A multilevel frequency-shift-keying (FH-MFSK) spread-spectrum communication system has been recently proposed[1] for cellular mobile-radio telephony. This system appears to perform better than other FH-DPSK systems, first proposed in Reference 2, when only one isolated cell is considered. However, a more realistic assessment of the FH-MFSK system calls for an analysis of its performance in a multicell context. An attempt to evaluate the number of simultaneous users that could be handled at a bit error rate of 10^{-3} was undertaken in Reference 3. In this paper[3] a mobile-to-base transmission model was proposed and system impairments such as intracell interference from nonsynchronous users and adjacent frequency channels in the presence of matched tuned receiver filters were analysed. For intercell interference, a Gaussian approximation was used and only qualitative results were given without any quantitative assessment being presented so far.

In this letter we present a computer simulation of the FH-MFSK transmission model mentioned[3] above, allowing a more precise evaluation of the number of simultaneous users that the system can tolerate when intercell interference is considered.

Monte Carlo simulation: It was shown in Reference 1 that the system bit error rate P_b could be readily obtained from the insertion probability P_I and miss probability P_{MISS}. These values were formulated in Reference 3 as

$$P_I = \text{prob}\,(|r(\tau) + I_{IC}(\tau) + n_f(\tau)| \geq C_0)$$

and

$$P_{MISS} = \text{prob}\,(|Re^{-j\theta}S_0(\tau) + r(\tau) + I_{IC}(\tau) + n_f(\tau)| < C_0)$$

where τ is the sampling time, $r(t)$ is the intracell interference signal, $n_f(t)$ is the received Gaussian noise, C_0 is a threshold decision value, $Re^{-j\theta}S_0(t)$ is the desired signal,

$$S_0(t) = \begin{cases} t & 0 < t < \tau \\ -t + 2\tau & \tau \leq t < 2\tau \end{cases}$$

R and θ are random variables, namely the Rayleigh and uniform distributions, respectively, and $I_{IC}(t)$ is the intercell interference. Details about the nature of $r(t)$ and $I_{IC}(t)$ are given in Reference 3.

The above formulas are maintained if clustering is used, but in this case the bandwidth available to each cell is the whole bandwidth available divided by the number of hexagonal cells which compose a single cluster (see Fig. 1).

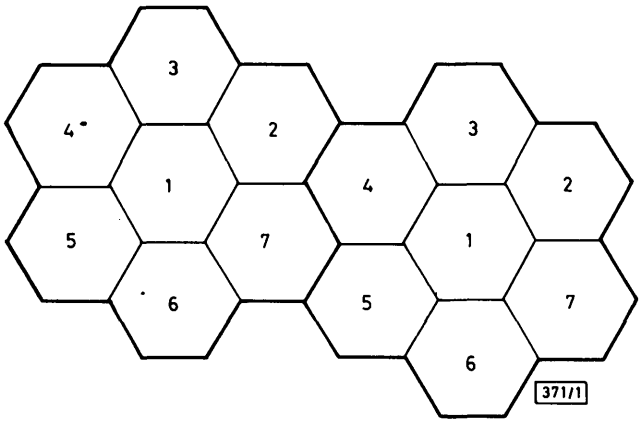

Fig. 1 *Hexagonal cell layout with clusters of seven cells*

The behaviour of P_I and P_{MISS} can be readily determined by Monte Carlo trials. It is merely necessary to generate independent uniformly distributed variables; then, by using the adequate transformations, samplings of $r(\tau)$, $n_f(\tau)$, $I_{IC}(\tau)$ and $Re^{-j\theta}S_0(\tau)$ can be obtained. This process is repeated N times, and ultimately we have

$$P_I \simeq \frac{\sum_{i=1}^{N} T_i}{N}$$

where

$$T_i = \begin{cases} 1 & \text{if } |r(\tau) + I_{IC}(\tau) + n_f(\tau)| \geq C_0 \\ 0 & \text{otherwise} \end{cases}$$

$$P_{MISS} \simeq \frac{\sum_{i=1}^{N} V_i}{N}$$

where

$$V_i = \begin{cases} 1 & \text{if } |Re^{-j\theta}S_0(\tau) + r(\tau) + I_{IC}(\tau) + n_f(\tau)| \leq C_0 \\ 0 & \text{otherwise} \end{cases}$$

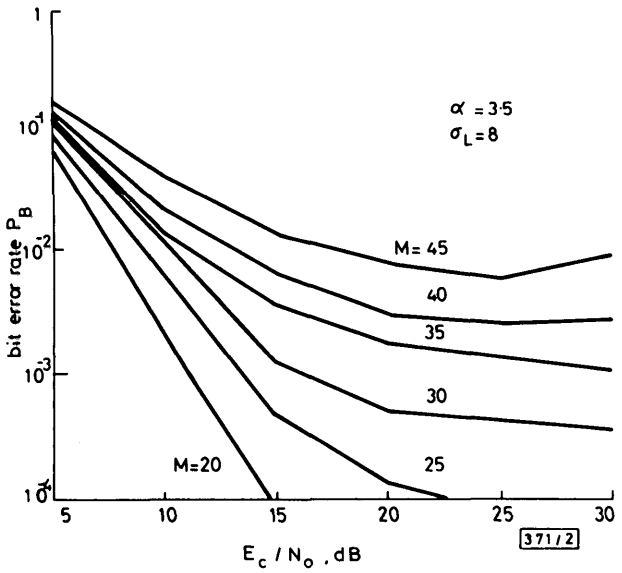

Fig. 2 *Bit error rate in a multicell system from Monte Carlo simulation*

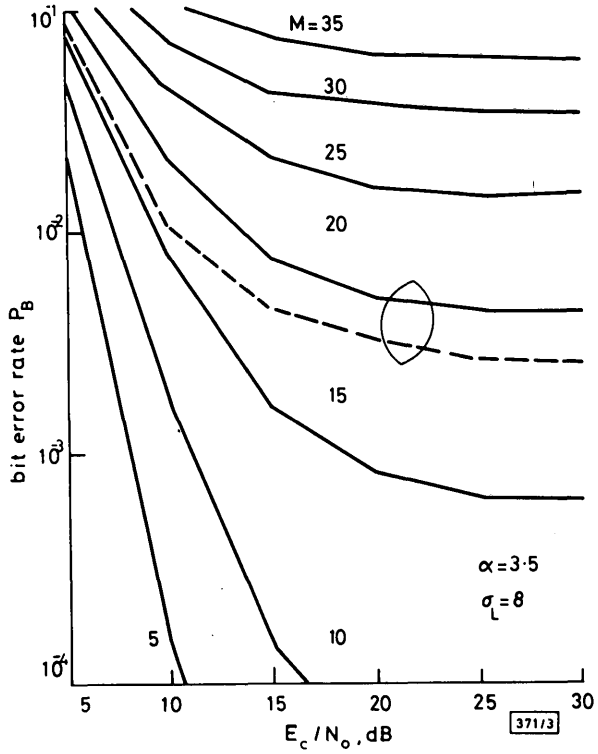

Fig. 3 *Bit error rate in a multicell system assuming Gaussian interference (dots represent Monte Carlo simulation points)*

$N = 10000$ was taken. Increasing this value produced a negligible change in the results but markedly increased run time. It can be observed that there may be some question regarding the accuracy of these results, particularly for P_b values smaller than 10^{-3}. Fortunately these P_b values are not usually handled in mobile-radio telephony.

Results: Fig. 2 shows the FH-MFSK system performance in the presence of six adjacent interfering cells. Every hexagonal cell contains M simultaneous users, the transmission rate per user is 32 kbit/s, and the bandwidth considered in each cell is the whole 20 MHz available. Power control in the mobiles, a mean path loss exponent α of $-3{\cdot}5$ and a lognormal distribution modelling the shadow fading with 8 dB standard deviation have been taken into account. Finally, optimum threshold decision values were found at each signal/noise ratio.

Fig. 3 shows the results obtained in Reference 3 by using the Gaussian approximation of the intercell interference. Comparing Figs. 2 and 3 leads to the realisation that the Gaussian approach is too pessimistic and a better performance could be expected. The dotted line of Fig. 3 also shows the FH-MFSK system performance using the Monte Carlo simulation and the Gaussian approximation of the intercell interference for $M = 20$ simultaneous users per cell. This analysis serves as a check on the validity of the Monte Carlo techniques.

In Reference 3 clustering was suggested as a strategy to improve the multicell performance. In order to gain insight on

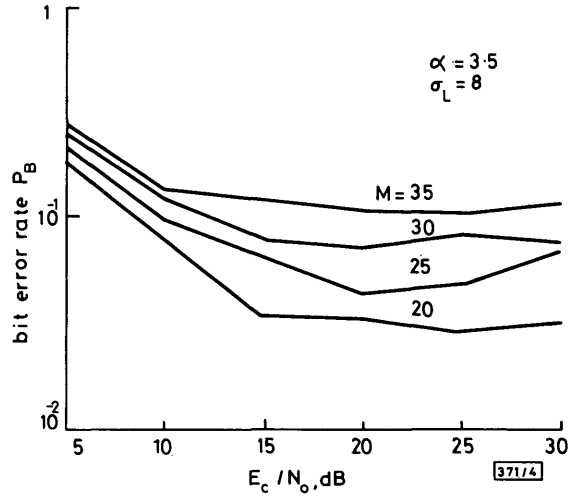

Fig. 4 *Bit error rate in a multicell system with a cluster of seven cells*

its effects, the desired cell and its six adjacent ones were considered to be a cluster or basic cell of repetition. The other clusters appearing in the multicell system were not taken into account because in a first approach the intercell interference arising with the clustering strategy was supposed negligible. The results plotted in Fig. 4 show that clustering worsens the multicell efficiency and consequently its presence in the FH-MFSK system is apparently not to be recommended. The indication is that the gains from spread-spectrum processing are offset by increased intracell interference, when this factor is taken into account.

R. AGUSTI-COMES
F. CASADEVALL-PALACIO
G. JUNYENT-GIRALT
ETSI Telecomunicación
Apdo. 30 002, Barcelona, Spain

31st October 1983

References

1 GOODMAN, D. J., HENRY, P. S., and PRABHU, V. K.: 'Frequency-hopped multilevel FSK for mobile radio', *Bell Syst. Tech. J.*, 1980, **59**, pp. 1257–1275
2 COOPER, G. R., and NETTLETON, R. W.: 'A spread spectrum technique for high-capacity mobile communications', *IEEE Trans.*, 1978, **VT-27**, pp. 264–275
3 AGUSTI, R., and JUNYENT, G.: 'Performance of FH multilevel FSK for mobile radio in an interference environment', *ibid.*, 1983, **COM-31**, pp. 840–846

MODE PARTITION NOISE CAUSED BY WAVELENGTH-DEPENDENT ATTENUATION IN LIGHTWAVE SYSTEMS

Indexing terms: Lasers and applications, Laser diodes, Optical transmission

Power fluctuations among the longitudinal modes of laser diodes cause noise in the received signal after being filtered by a wavelength-dependent attenuation mechanism. We have developed a theoretical model to characterise this noise and studied degradation in lightwave system performance. Power penalties observed in a 432 Mbit/s wavelength division multiplexing system experiment agreed with theoretical predictions.

Mode partition noise (MPN) in lightwave systems is caused by a combination of instantaneous fluctuation of the power distributed among the laser modes and spectral filtering in the transmission path. MPN associated with fibre dispersion causing phase delay in each pulse has been extensively discussed in the literature[1] and found to set one of the performance limitations in high-bit-rate lightwave systems.

In this letter we describe MPN caused by wavelength-dependent attenuation in the transmission path.[2] MPN of this kind is especially important in designing WDM systems, where transmission characteristics near cutoff wavelengths of multiplexers and demultiplexers are highly wavelength-dependent. Wavelength-dependent fibre attenuation in long-haul systems also can cause this type of MPN in addition to the MPN associated with fibre dispersion, especially in system channels operating near the OH absorption peaks.

Let a_i and f_i represent the instantaneous power in the laser's ith mode and mode-dependent attenuation in the transmission path at wavelength λ_i, respectively. Then the signal amplitude of each pulse arriving at the receiver can be given by

$$S = \sum_i a_i f_i \tag{1}$$

Assuming that the power is normalised such that $\sum_i a_i = 1$ and that the partitioning is constant over the duration of each pulse but random from pulse to pulse, MPN can be described using the average value and the variance of the received signal as[3]

$$\sigma_n^2 = k^2 \sum_i \sum_{j>i} (f_i - f_j)^2 \bar{a}_i \bar{a}_j \tag{2}$$

where $\bar{a}_i$ represents time-averaged power of the ith mode and mode partition coefficient k represents a measure of the power which fluctuates. The coefficient k is assumed to be constant for all modes. The noise-to-signal ratio due to MPN can be given by

$$N/S = \sigma_p^2 = \sigma_n^2/\bar{S}^2 \tag{3}$$

The power penalty ΔP, which is defined as the increase in received power necessary to maintain an error rate equal to the one without MPN, is then given by

$$\Delta P(\text{dB}) = -5 \log_{10} (1 - Q^2/Q_c^2) \tag{4}$$

where $Q_c = 1/\sigma_p$ and Q is the Q-value associated with a given bit error rate.[4]

Although eqns. 2–4 can be calculated numerically for a given laser spectrum and filtering characteristic, it is useful to obtain an analytical formula to evaluate system performance by making the following assumptions.

The time-averaged envelope of the laser spectrum is approximated with a Gaussian centred at wavelength λ_c and of half-width $\Delta\lambda$:

$$a(\lambda) = \frac{1}{\Delta\lambda\sqrt{2\pi}} \exp\left[-(\lambda - \lambda_c)^2/2(\Delta\lambda)^2\right] \tag{5}$$

The wavelength-dependent attenuation is assumed to be linear with wavelength around λ_c:

$$f(\lambda) = \tfrac{1}{2} \exp\left[-A(\lambda - \lambda_c)/4{\cdot}34\right] \tag{6}$$

where A represents rate of attenuation change in dB/nm. Substituting eqns. 5 and 6 into eqns. 2 and 3 and approximating the sums with integrals yields

$$\sigma_p^2 = k^2(\exp\left[(A\ \Delta\lambda/4{\cdot}34)^2\right] - 1) \tag{7}$$

and from eqn. 4 the power penalty is given by

$$\Delta P = -5 \log_{10} \{1 - Q^2k^2(\exp\left[(A\ \Delta\lambda/4{\cdot}34)^2\right] - 1)\} \tag{8}$$

Transmission degradation due to MPN was investigated experimentally as the optical signal was sent through a grating demultiplexer used for a single-mode two-channel WDM system experiment.[5,6] The power penalties due to MPN were determined from bit error rate (BER) against received power measurements with and without the demultiplexer. Buried-heterostructure (BH) InGaAsP/InP lasers were modulated with 432 Mbit/s NRZ format. Fig. 1 shows the spectral attenuation of the grating demultiplexer and the operating wavelengths of laser transmitters.

Table 1 summarises laser spectra and transmission filtering characteristics. Also given are MPN penalties measured at

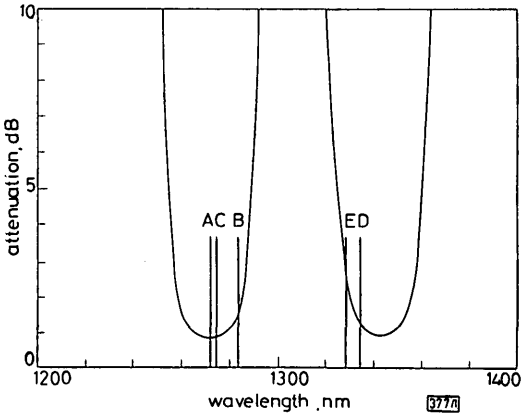

Fig. 1 *Spectral attenuation of grating demultiplexer and laser operating wavelengths*